Earthquakes and Structures, *Vol. 11, No. 1 (2016) 83-107*
DOI: http://dx.doi.org/10.12989/eas.2016.11.1.083

Vibration response of saturated sand - foundation system

Mohammed Y. Fattah[*1], Mosa J. Al-Mosawi[2a] and Abbas F.I. Al-Ameri[2b]

[1]*Building and Construction Engineering Department, University of Technology, Baghdad, Iraq*
[2]*College of Engineering University of Baghdad, Iraq*

(Received June 12, 2015, Revised May 26, 2016, Accepted June 10, 2016)

Abstract. In this study, the response and behavior of machine foundations resting on dry and saturated sand was investigated experimentally. A physical model was manufactured to simulate steady state harmonic load applied on a footing resting on sandy soil at different operating frequencies. Total of (84) physical models were performed. The parameters that were taken into consideration include loading frequency, size of footing and different soil conditions. The footing parameters are related to the size of the rectangular footing and depth of embedment. Two sizes of rectangular steel model footing were used. The footings were tested by changing all parameters at the surface and at 50 mm depth below model surface. Meanwhile, the investigated parameters of the soil condition include dry and saturated sand for two relative densities; 30 % and 80 %. The dynamic loading was applied at different operating frequencies. The response of the footing was elaborated by measuring the amplitude of displacement using the vibration meter. The response of the soil to dynamic loading includes measuring the stresses inside soil media by using piezoelectric sensors.

It was concluded that the final settlement (St) of the foundation increases with increasing the amplitude of dynamic force, operating frequency and degree of saturation. Meanwhile, it decreases with increasing the relative density of sand, modulus of elasticity and embedding inside soils. The maximum displacement amplitude exhibits its maximum value at the resonance frequency, which is found to be about 33.34 to 41.67 Hz. In general, embedment of footing in sandy soils leads to a beneficial reduction in dynamic response (displacement and excess pore water pressure) for all soil types in different percentages accompanied by an increase in soil strength.

Keywords: dynamic; saturated soil; machine foundation; displacement

1. Introduction

Machine foundations are regarded as the most important elements of industrial structures like power plants, steel plants, petrochemical complexes, and fertilizer plants etc. It consists of a number of reciprocating and centrifugal machines which play an important part in ensuring efficient performing of the process, and that the output product is of the required quality. If any of these parts starts functioning or breaks down due to disproportion at vibration or large settlement of the foundations, this may lead to catastrophic performance requirements at certain times

*Corresponding author, Professor, E-mail: myf_1968@yahoo.com
[a]Professor, E-mail: prof_mosa_2006@yahoo.com
[b]Lecturer, E-mail: alameri.abbas@gmail.com

http://www.techno-press.com/journals/eas&subpage=7 ISSN: 2092-7614 (Print), 2092-7622 (Online)

(Chowdhury and Dasgupta 2010).

Different factors have major influence on the behavior of the machine foundations, such as dynamic properties of soil that support the foundation, weight of the foundation and vibrating equipment, contact area of foundation with soil, static soil pressure, nature and magnitude of unbalanced force. The complexity of dynamic loading in nature as well as the non-homogeneity of soil makes the analysis and design of foundations subjected to dynamic load to be complex (Ramesh and Kumar 2011).

Al-Homoud and Al-Maaitah (1996) found that there is an increase in natural frequency and a reduction in amplitude with the increase in degree of saturation of sandy soil subjected to vertical forced vibration loading. On the other hand, for free vibration test, the results showed that for different footing models resting on sandy soil, there is an increase in damping ratio with increase in the degree of saturation, as well as the damping ratio of footing on saturated sand is higher than that on dry sand.

Xiaobing *et al*. (2004) studied the influence of the vertical vibration loading on the liquefaction of saturated sand. They presented one-dimensional model for the saturated sand with a vertical vibration based on the two-phase continuous media theory. Based on their numerical modeling, they concluded that the saturated sand may liquefy under vertical vibration loading. Furthermore, (Lu and Cui 2004) studied the water wave induced liquefaction in highly saturated sand, it was found that the non uniform permeability possesses great effect on the generated pore water pressure during vibrations.

Boumekik *et al*. (2010) performed laboratory tests to estimate soil dynamic stress induced by a vibrating foundation prototype for three specific points of the foundation-soil interface zone. It was concluded that the testing prototype gives satisfying results for simulating a superficial foundation behavior under a cyclic and dynamic loading. It was found that an increase in the density of the medium dense sand due to the particle retightening at the central zone level leads to an increase in its density. In the dense sand case, the axial overstresses would have the tendency to be transmitted to the corners because of the initial confinement.

Fattah *et al*. (2011) mentioned that extensive research has been performed in which laboratory specimens of saturated sand were subjected to either controlled cyclic stresses or strains. The equipment used was triaxial, simple shear, hollow torsional, shaking table, and centrifuge. Different variables have been investigated including density of sand, confining pressure, frequency of loading, shape of load cycle, method of sample preparation and cyclic loading history. It was found that as a consequence of applied cyclic stresses, the structure of the cohesionless soil tends to become more compact with a resulting transfer of stress to the pore water and a reduction in stress on the soil grains. As a result, the soil grain structure rebounds to the extent required keeping the volume constant, and this interplay of volume reduction and soil structure rebound determines the magnitude of the increase in pore water pressure in the soil.

Fattah *et al*. (2013) from finite element analysis, found that for loose sand, initial cyclic pore water pressure induced softening leads to monotonic accumulation of shear deformation but when the soil density increases, a reduction in the rate of generation of pore water pressure occurs. On the other hand, for loose sand, there is no change in pore water pressure due to increase in the load amplitude, which takes place after the initial liquefaction has occurred but when the sand densifies, a limited increase, or (sometimes a slight decrease) occurred in pore water pressure because of increasing of load amplitude.

2. Soil-Structure Interaction (SSI)

In the last twenty years, structures and foundations were in complete isolation where the structural and geotechnical allocated foundation engineers hardly interacted (Chowdhury and Dasgupta 2010). With the great and dramatic changes in the computer science, the SSI received considerable attention and solving complex problem became possible.

There are different types of problems that go into the definition of soil-structure interaction, such as footing (shallow and deep), dams, retaining and buried structures, etc. The solution of the dynamic soil structure interaction (DSSI) problems can be achieved using the following approaches:

1. Equivalent soil springs connected to foundations modeled as beams, plates, shell etc.,
2. Finite element models (mostly used in 2D problems),
3. Mixed finite element and boundary element: a concept that is slowly gaining popularity.

Christian and Hall (1982) and Han (2010) explained that the analysis of the dynamic interaction of soils and structures changes substantially as the specific physical problem changes. There are at least four dynamic soil-structure interaction problems:

1. Vibrating machinery is relatively small compared to the extent of the founding soil, and the important conditions are usually those during continuous operation of the equipment. Therefore, a steady state solution for a structure found at or near the surface of a half-space is usually satisfactory.
2. Blast monitoring or blast protection involves a transient problem with very few, usually one, pulses of overpressure. Steady state response and the behavior at large times are not especially important.
3. Earthquakes involve long input signals that have rich frequency contents and many cycles of load reversal. Because the waves propagate over a considerable distance, the modeling of large and complicated geometries is an important issue. The input motion is often not well known and is often specified at an unknown or inconvenient location.
4. Large offshore structures experience some transient response, but the steady state response to wave loading is most significant for fatigue problems.

Omidvar *et al*. (2012) developed a three-dimensional hybrid model for the analysis of soil-structure interaction under dynamic conditions. The modeling was achieved by partitioning the total soil-structure system into a near field and a field with a hemispherical interface. The near field was simulated by the finite element method. The semi-infinite field was modeled by distributed impedance function at the interface, which was determined by system, which made possible realistic and economical assessment of three-dimensional soil-structure interaction for both surface and embedded structures.

An analytical formulation was presented by Omidvar *et al*. (2012) to analyze the case of an axially loaded rigid cylindrical rod partially embedded in an elastic half-space. The problem was formulated by means of Hankel integral transforms and reduced to systems of coupled singular integral equation, where the unknown quantities are the normal and shear stresses acting along the contact surface.

Messioud *et al*. (2016) analyzed the seismic response of a three-dimensional (3-D) rigid massless square foundation resting or embedded in a viscoelastic soil limited by rigid bedrock. The foundation was subjected to harmonic oblique seismic waves P, SV, SH and R. The key step was the characterization of the soil-foundation interaction by computing the impedance matrix and the input motion matrix. A 3-D frequency boundary element method (BEM) in conjunction with the thin layer method (TLM) was adapted for the seismic analysis of the foundation. The dynamic response of the rigid foundation was solved from the wave equations by taking into account the soil-foundation interaction.

In addition to the above-mentioned works, there are many researchers whose analytical approaches take into consideration different types of analysis, modeling, and techniques. This may give a clear idea for the complexity of the DSSI as well as its dependency on the soil, structure, and foundation properties.

From the available literature related to the machine foundation analysis and design, it could be concluded that different parameters and factors might affect the performance of machine foundation. The main points that can be highlighted from literature review are:

1. The behavior of foundation subjected to dynamic loads is highly dependent on the type of machine as well as operating frequency, soil state, depth of embedment and method of analysis.
2. The response of supporting soil to the machine foundation is affected by different parameters such as amplitude of loading, geometry of footing, soil state and condition, type of dynamic loading etc.
3. The modeling of soil subjected to dynamic loading is highly dependent on the level of induced strain. Hence, the sandy soil can be modeled as linear elastic material in dynamic analysis since the resulting strain is always less than 10^{-4}.

The main objectives of this paper are to study the effect of steady state harmonic loading on the response of foundation-soil system. To achieve the main objectives of the research, different steps and minor objectives are performed as listed below:

• Studying the effect of foundation geometry and depth of embedment on the dynamic response of machine foundations on dry and saturated sandy soil with different densities.

• Studying the effect of dynamic load amplitude on the dynamic response of soil and machine foundation.

3. Experimental work

Several methods are available to determine the displacement amplitude of the machine foundations. Most of these methods consider the underlying soil to being in dry state. In this section, small-scale experiments are performed to simulate a physical model of machine foundation on dry and saturated soil.

In the case under consideration of machine foundation, the dynamic system is the soil media through which waves propagate outward from sources of machine vibrations. The input signal of the system is the impulse response of the ground at the place of installation of a machine foundation; the output signal is the dynamic response of a location of interest situated on any point at a foundation receiving vibrations or within the soil stratum.

All the tests were performed in the laboratories of the College of Engineering in Baghdad University. The total number of the tests carried out is 84 models. In general, the testing program consists of two major parts. The first part is devoted to dry sand models with total number of tests of 56. The tests were performed in loose and dense soil state. Two footing sizes and the models were tested at the surface of the footing and at a depth of 5.0 cm. The second part is concerned with saturated sand models with total number of 28 models. The same parameters were taken into consideration except that the models were prepared from dense sand only. The details of abbreviation for the tested samples as well as example of models naming are explained below.

D or S	L or D	10	20	S or E
Sand conditions (dry or saturated)	**Sand state (Loose or dense)**	**Width of the model footing 10 or 20 cm**	**Length of the model footing 20 or 40 cm**	**Depth of footing 0.0 or embedded at 5.0 cm**
DL1020S: Dry loose state sand, footing 10×20 cm, footing placed at the surface.				
SD2040E: Saturated dense state sand, footing 20×40 cm, footing embedded at 5.0 cm below surface.				

The physical model set up is shown in Fig. 1. Descriptive sketches of the test equipment, measuring devices and tools are presented in Fig. 2.

4. Description of testing components

A series of model loading tests were conducted inside a rigid steel box of dimensions (1200×1000×600 mm), made of steel plate of 5.0 mm thickness. These dimensions were chosen to satisfy the boundary effects of physical models subjected to dynamic loading. The overall description of test components and measuring devices is shown in Fig. 1.

The dynamic response was evaluated by taking the measurements of displacement amplitude and the final settlement. To create a physical model, a small container was manufactured from steel plate. The container, which has the dimensions of (length 1200 mm, width 1000 mm and height 600 mm), was used to prepare the bed of soil. The tested soil is clean sand passing through

Fig. 1 General view of the testing models and instruments

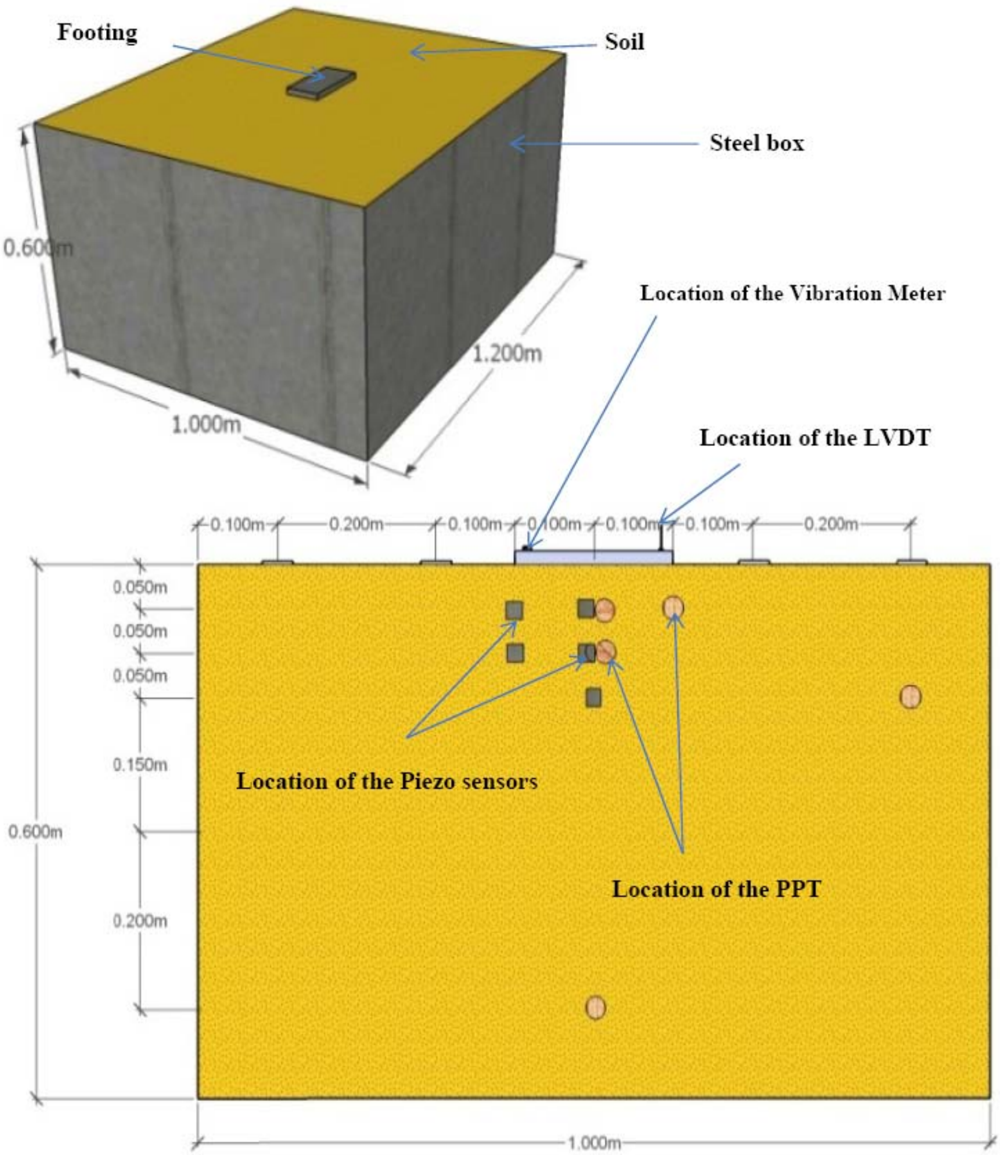

Fig. 2 Schematic view of the sand model and instruments layout

ASTM standard sieve No.10 (2.0 mm) and retained on the ASTM standard sieve No. 100 (0.150 mm) to obtain uniform sand. The required amount of the prepared soil was placed into the steel container in different layers with a uniform density and then saturated with water.

Two alloy steel model footings of size (200×100×12.5) mm and (400×200×5.0) mm were placed centrally over the prepared soil layer, and then a mechanical oscillator was fixed to the footing to act as a single unit. The size of the footing was chosen to obtain rigid footing.

The foundation was subjected to vibration in the vertical direction. The frequency and corresponding displacement amplitude of vibration were measured. A sufficient time between two successive measurements was given to reach steady state, which facilitates accurate measurement of frequency and the corresponding displacement amplitude. The used equipment can be classified into two categories; one is required for inducing a known pattern of vibration (sinusoidal waveform) and the other is required for measuring the vibration response.

Soil can commonly be considered as a semi-infinite media. In the horizontal direction, it can often be regarded as infinite, therefore allows the continuous dissipation of energy without disturbance. In the present model, special boundary conditions were adopted by using cork (styropor) sheets of 40.0 mm thickness. These sheets would satisfy two main points:

- The styropor cork sheets can reduce the slight friction that might be developed between the box faces and soil.
- It works as absorbing boundaries to prevent reflected waves.

Preliminary tests were performed to check the efficiency of such materials as boundary absorbing purposes. This approach was achieved by measuring the dynamic response at the boundaries with and without absorbing layers. It was found that the using of the flexible synthetic material (styroporcork sheets) has good damping properties, which insure the using of such material as absorbing layer is efficient.

5. Sample preparation

Tamping and pouring procedures were used to prepare the sandy soil inside the steel box. This method was followed to ensure the desired relative density as well as to ensure the same method of sample preparation in loose and dense state. In addition to that, hygroscopic water content (≈0.5-3.0%) was added to the sand prior to compaction and pouring to ensure small cementation of soil before testing. This water content is regarded as uncontrolled water content that is always present within the sample without oven drying.

For the loose state sand models, the sample was prepared by pouring the soil inside the box from a certain height. The hygroscopic water content for loose state was about 0.5-1.0%. The suitable height was decided by making a relation between the height of falling and the resulting dry density. It was found that a 30 cm falling height gives the desired value of dry density. For the sake of accuracy and reducing the sources of sample disturbance, the box was divided into sub layers of 50.0 mm. Filling operation throughout the test was performed using galvanized metal hopper with height of 30 cm having a valve to control sand raining by hand.

On the other hand, for dense state soil models, hygroscopic water content of (2.0-3.0%) was added to the sample to ensure compactness and cementation of soil within the model. The box was divided into sublayers of about 50 mm thickness, each layer was compacted using standard hammer.

After sample preparation commenced, the density was checked using sand balloon for field density test according to (ASTM D2167-08) specification. The variation of the resulting density was ±5 %. This variation is considered acceptable.

For preparation of saturated models, the soil was saturated by pouring a known minimum quantity of water that is required for saturation. This quantity of water was calculated from the basic relations in soil mechanics. For achieving permanent saturation of sand, additional water was added to the sample prior to test. Care was taken to ensure that no water could be draining out from the steel box.

6. Soil used

The physical properties of sand used include specific gravity, grain size distribution and the maximum and minimum dry unit weights of the sand. A summary of the test results with standard specification following each test is presented in Table 1.

Table 1 Physical and mechanical properties of the used sand

Property			Value	Standard of the test
Specific Gravity, Gs			2.65	ASTM D 854
Gravel (>4.75 mm)%			0	ASTM D 422 and ASTM D 2487
Sand (0.075-4.75 mm)%			96	
Silt and clay (<0.075 mm)%			4	
Coefficient of curvature, Cc			1.55	
Coefficient of uniformity, Cu			1.73	
D_{10}, D_{30}, D_{60} (mm)			0.11, 0.18, 0.19	
USCS-soil type			SP	
Dense state relative density, Dr, %			80.0	
Loose state relative density, Dr, %			30.0	
Maximum dry unit weight, γ_{dmax}, kN/m^3			18.2	ASTM D 4253-00
Minimum dry unit weight, γ_{dmin}, kN/m^3			14.3	ASTM D 4254-00
Dry unit weight in loose state (Used), kN/m^3			15.4	------
Dry unit weight in dense state (Used), kN/m^3			17.3	------
Angle of internal friction, ϕ	Loose state (30%)	Dry	28.0	ASTM D 3080
		Soaked	26.0	
	Dense state (80%)	Dry	40.0	
		Soaked	36.0	
Coefficient of permeability, k, m/sec		Loose state (30%)	0.0360	ASTM D2434-68
		Dense state (80%)	0.0065	

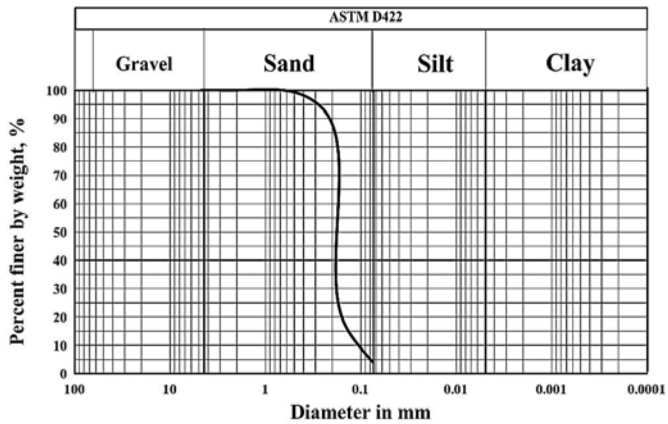

Fig. 3 The grain size distribution curve of the used sand

According to the grain size distribution curve results presented in Fig. 3, it can be seen that the sand is of medium to coarse size. According to the Unified Soil Classification System (USCS), the sand is classified as (SP) and described as poorly graded sand.

It is important to state herein that the sand used in the physical models passes through sieve No. 10 and retains on sieve No. 100. Therefore, the mechanical properties of the sand in loose and dense state as well as in dry and saturated conditions were tested. The angle of internal friction was measured through direct shear test following ASTM D 3080 specification for both dry and soaked samples. In addition, traditional unconsolidated undrained triaxial test was carried out on dry samples to get reliable values of the modulus of elasticity. This test was carried out according to ASTM D2850 specification. The coefficient of permeability of the soil is determined by using the constant-head permeability test according to ASTM D2434 specification in dense and loose states. The results of these tests are summarized in Table 1.

7. Equipment for inducing vertical vibration

In this study, systematic experiments were performed to investigate the dynamic response of foundation on a dry and saturated soil under the effect of harmonic vertical mode of vibration. The vertical vibration tests were conducted to simulate different values of dynamic loads using mechanical oscillator with different frequencies and eccentric settings. A total number of seven frequencies are adopted in this study. Each frequency represents certain amplitude of dynamic force. At each operating speed, different cases and parameters related to footing and soil have been studied.

The principle of this equipment is the vibrator that is also called the oscillator. The model machine of the mechanical oscillator used in this study is shown in Fig. 4. The mechanical oscillator consists of a rotating disc manufactured from steel with diameter 54 mm and thickness 5.1 mm. A single mass (m_e) is placed on the rotating disc at an eccentricity of 22 mm from the axis of rotation. This arrangement rotates in one direction when it is driven through a shaft by an AC motor having a maximum rated speed of up to 3500 rpm. Such an arrangement induces a vibratory force at the base of the oscillator. This vibratory force can be estimated from Eq. (1). In this study, the vibration force-time history (reaction force-time history) was measured during the test.

The basic principle of this device can be found in different textbooks such as Bhatia (2009). Depending on the orientation of the counter-rotating shaft, a vertical dynamic force can be applied. The amplitude of vertical force produced (F_o) is

$$F_o = m_e . e . \omega_r^2 \tag{1}$$

where:

ω_r is the circular operating frequency of the machine,

e is the eccentric distance from the shaft to the unbalanced mass me, and

m_e is the unbalanced mass.

For this type of oscillator, the function of the harmonic vertical mode of vibration is sinusoidal. Therefore, the applied dynamic force $F(t)$, at any time (t) is given by

$$F(t) = F_o . \sin \ \omega_r . t = m_e . e . \omega_r^2 . \sin \omega_r . t \tag{2}$$

The most challenge in this type of vibratory machine is how to control the speed of the motor? In this research, a special AC Drive was used to control the speed of rotation. Calibration of this

(a) Location of the eccentric mass

(b) Dynamic load cell

Fig. 4 Equipment for inducing vibratory dynamic load

device with Tachometer was done to check the accuracy of the AC Drive. By varying the voltage supplied to the motor with the aid of the speed AC Drive, the speed of the motor and hence the oscillator can be varied which, in turn, causes a change in frequency of vibration induced by the oscillator.

8. Dynamic load measurement (F-t History)

As mentioned before, the harmonic reaction force-time history was measured during the test. For measuring the vibration force, a dynamic load cell was used specially for this purpose. The dynamic load cell was MLC215C-3T supported with MEP105Aweighing indicator (Manyear Technology Company Limited 2011).

For obtaining high sensitivity of readings, the output lead wires of the dynamic load cell were connected to the Vishay Digital Strain Indicator that was provided with an analog output. The output signal from the strain indicator was captured by using a digital storage oscilloscope TWINTEX (TSO 1202, 200MHz) and then connected to data acquisition system by laptop computer device as shown in Fig. 1.

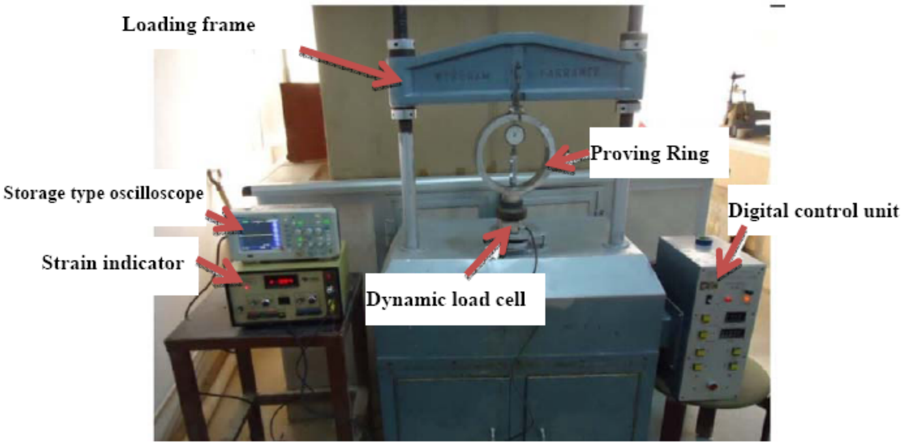

Fig. 5 Calibration of dynamic load cell during loading using controlled compression machine

The operation of storage type oscilloscope was enhanced with computer interface system that makes it more familiar to the computer uses. The load cell was calibrated by using a (10 ton capacity) compression machine with proving ring capacity of (10 ton). High rate of load application (5.0 mm/min) was used with the dynamic load cell and the output voltage was recorded during loading by using storage type oscilloscope. The general view of calibration is shown in Fig. 5.

The dynamic load applied to the footing was measured using dynamic load cell. This measurement can be regarded as the reaction force resulting from the applied load. It was found that the reaction force depends on the relative density of the soil.

9. Measurement of the amplitude of footing displacement

The vertical amplitude of footing (Az) was measured at the surface of the footing. Vibration meter (HG 6360) of one channel was used in the test. This vibration meter has a working capacity of 0.001 to 4.0 mm, it is capable of measuring the displacement, velocity, and acceleration of motion depending on the function set prior to the test. In addition, all the collected data can be transferred to the computer easily through built in software. During the tests, one vibration meter was used on the surface of the footing. The components of the HG 6360 vibration meter are shown in Fig. 6. The vibration meter within the testing models is shown in Fig. 1.

10. Data acquisition system (DAS)

Displacement amplitude of footing, pore water pressure and the reaction force-time history were measured using a mobile data acquisition system. The data acquisition system used in this study includes Laptop computer, one channel strain indicator (which can receive data from the load cell attached to the footing surface) and piezoelectric sensors. The general view of the data acquisition system is shown in Fig. 1. All these instruments were connected to the storage type

Fig. 6 Components and position of the HG 6360-vibration meter of the HG

oscilloscope, which is fully compatible with computer output purposes. By using the storage type oscilloscope with any piezoelectric sensor, indicator, or load cell, the scanning process and triggering of the data can be controlled by the user according to the required accuracy and rate of readings.

On the other hand, the vibration meter is accompanied by software that is based on Lab view software sufficient to acquire and store the data for each test and save the data in text files automatically.

11. Presentation and discussion of experimental test results

The presentation includes the 84 model tests, performed on dry and saturated sand subjected to vertical dynamic loading at loose and dense state relative densities. The size of the footing and depth of embedment were investigated. The investigation focused on the influence of the amplitude of loading, relative density of sand bed, size of footing and depth of embedment and different dynamic response parameters. The model tests can be divided into two main parts:

1. The first part consists of 56 models performed on dry sand, and
2. The second part consists of 28 models performed on saturated dense sand. It is valuable to state herein that the loose state sand models for saturated condition were not tested in this study, because the soil fails immediately when the model machine is switched on.

12. Final settlement and displacement amplitude

12.1 Total settlement of footing

The total or final settlement (St) of the footing resulting from the dynamic load subjected to the footing was measured. The measurement of settlement was done by using the LVDT at the end of the test. The test results are drawn in Figs. 7 to 9 and the summary of the test results is included in Table 2. To make a comparison between different soil model responses, Table 3 is prepared. This table contains the ratios of measured settlement between different models.

The measured settlement represents the final reduction in the thickness of the soil under the footing. This value was taken from the final reading of the LVDT postulated at the surface of the footing.

It is important to state herein that the time of the test was not less than three minutes unless the machine moves from its position during vibration. This happened for some models when the footing of (10×20 cm) size was tested on the surface under high operating frequency. The time of

Table 2 Summary of the displacement amplitude and total settlement for different test conditions

Test No.	Test condition	Operating frequency, ω_r, rpm	Az, mm	S_t, mm
1		500	0.0001	0.01
2		1000	0.0111	3.00
3		1500	0.0740	7.00
4	**DL1020S**	2000	0.1600	8.35
5		2500	0.5010	13.00
6		3000	0.1700	21.00
7		3500	0.1040	25.00
8		500	0.0030	0.00
9		1000	0.0162	0.30
10		1500	0.0572	0.80
11	**DL2040S**	2000	0.0961	1.55
12		2500	0.3010	2.15
13		3000	0.0970	3.60
14		3500	0.0601	7.00
15		500	0.0030	0.00
16		1000	0.0081	0.20
17		1500	0.0340	0.75
18	**DL1020E**	2000	0.0930	4.20
19		2500	0.1340	5.95
20		3000	0.0651	8.50
21		3500	0.0292	12.00
22		500	0.0040	0.05
23		1000	0.0030	0.10
24		1500	0.0071	0.10
25	**DL2040E**	2000	0.0310	1.10
26		2500	0.1120	1.70
27		3000	0.0580	2.55
28		3500	0.0110	5.45

Table 2 Continued

Test No.	Test condition	Operating frequency, ω_r, rpm	Az, mm	S_t, mm
29		500	0.0001	0.00
30		1000	0.0060	0.06
31		1500	0.0650	0.70
32	**DD1020S**	2000	0.1580	0.90
33		2500	0.1510	1.00
34		3000	0.0460	2.00
35		3500	0.0280	4.00
36		500	0.0001	0.00
37		1000	0.0010	0.05
38		1500	0.0060	0.10
39	**DD2040S**	2000	0.0907	0.60
40		2500	0.0792	0.70
41		3000	0.0380	0.75
42		3500	0.0173	0.90
43		500	0.0020	0.00
44		1000	0.0021	0.05
45		1500	0.0080	0.08
46	**DD1020E**	2000	0.0910	0.50
47		2500	0.0751	0.30
48		3000	0.0611	0.40
49		3500	0.0288	1.10
50		500	0.0010	0.00
51		1000	0.0014	0.00
52		1500	0.0040	0.00
53	**DD2040E**	2000	0.0300	0.05
54		2500	0.0270	0.10
55		3000	0.0056	0.15
56		3500	0.0070	0.25
57		500	0.0011	0.05
58		1000	0.0020	0.60
59		1500	0.0650	3.25
60	**SD1020S**	2000	0.3820	5.50
61		2500	0.1482	10.10
62		3000	0.0910	13.00
63		3500	0.0783	20.95
64		500	0.0010	0.05
65	**SD2040S**	1000	0.0033	-0.05
66		1500	0.0180	0.45

Table 2 Continued

Test No.	Test condition	Operating frequency, ω_r, rpm	Az, mm	S_t, mm
67	**SD2040S**	2000	0.2120	1.35
68		2500	0.0980	2.35
69		3000	0.0800	3.15
70		3500	0.0230	4.95
71	**SD1020E**	500	0.0250	0.10
72		1000	0.0411	0.50
73		1500	0.0940	0.85
74		2000	0.2780	0.90
75		2500	0.1802	2.25
76		3000	0.0480	4.75
77		3500	0.0250	7.00
78	**SD2040E**	500	0.0082	0.05
79		1000	0.0090	0.00
80		1500	0.0044	0.05
81		2000	0.2008	0.10
82		2500	0.2880	0.50
83		3000	0.0890	0.55
84		3500	0.0640	0.85

Table 3 Comparison ratios between the settlement measured for different footing sizes and soil conditions

ω_r rpm	$\left(\frac{\text{DL1020S}}{\text{DD1020S}}\right)$	$\left(\frac{\text{DL1020E}}{\text{DD1020E}}\right)$	$\left(\frac{\text{DLZ040S}}{\text{DDZ040S}}\right)$	$\left(\frac{\text{DLZ040E}}{\text{DDZ040E}}\right)$	$\left(\frac{\text{DD10Z0S}}{\text{SD10Z0S}}\right)$	$\left(\frac{\text{DLZ040S}}{\text{SDZ040S}}\right)$	$\left(\frac{\text{DD10Z0E}}{\text{SD10Z0E}}\right)$	$\left(\frac{\text{DDZ040E}}{\text{SDZ040E}}\right)$
500	>> 1.0	>> 1.0	>> 1.0	>> 1.0	0.00	0.00	0.00	0.00
1000	50.0	4.0	6.0	>> 1.0	0.10	1.00	0.10	1.00
1500	10.0	9.4	8.0	>> 1.0	0.22	0.22	0.09	0.00
2000	9.3	8.4	2.6	22.0	0.16	0.44	0.56	0.50
2500	13.0	19.8	3.1	17.0	0.10	0.30	0.13	0.20
3000	10.5	21.3	4.8	17.0	0.15	0.24	0.08	0.27
3500	6.3	10.9	7.8	21.8	0.19	0.18	0.16	0.29

operating the machine was two minutes, after that, the machine was switched off by powering off the motor and free vibration of the system was allowed.

In general, it was noticed that the sandy soil exhibited rebound, i.e., small part of settlement was recovered as the rotating machine shut down. Therefore, it is important to mention that the listed values of total settlement represent the settlement taken immediately as the rotating machine shutdown.

The test results show that the settlement increases with increasing the amplitude excitation force for all the tested models, as well as, the rate of settlement increase in loose sandy soil is

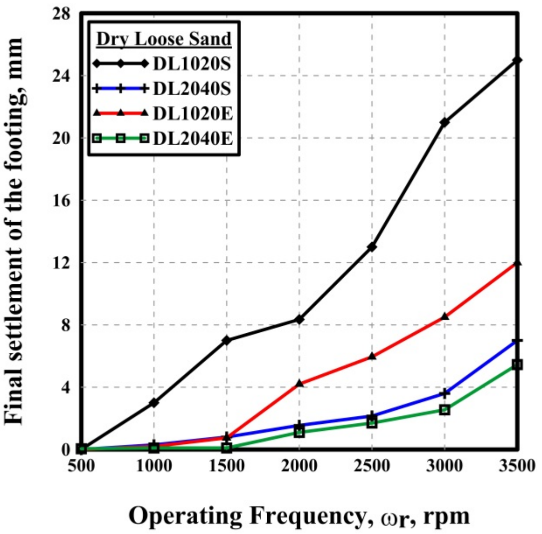

Fig. 7 Total settlement versus operating frequency relationship for dry loose sand

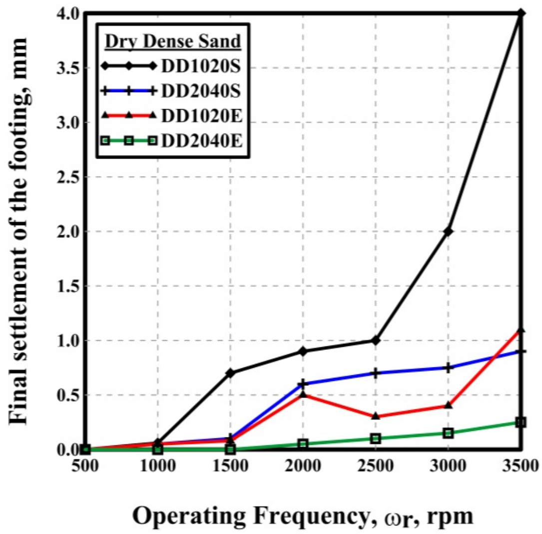

Fig. 8 Total settlement versus operating frequency relationship for dry dense sand

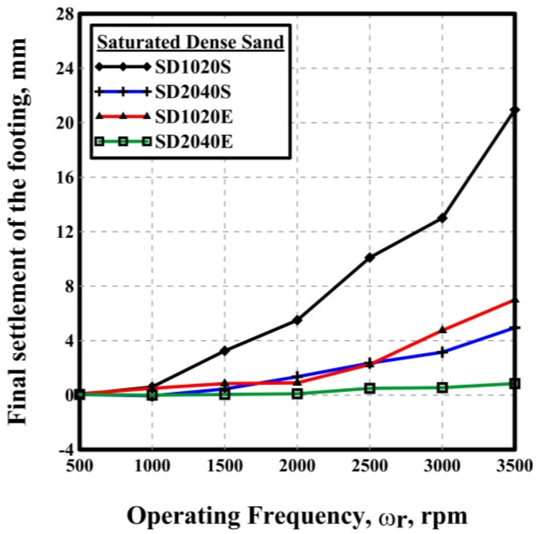

Fig. 9 Total settlement versus operating frequency relationship for saturated dense sand

greater than that of dense sandy soil.

With the exclusion of the test results at operating frequency of 500 rpm, the experimental model test results reveal that, the loose sand settles greater than the dense sand models. For footing placed at the surface, the ratio of dry loose sand settlement to dry dense sand settlement is ranging from (6.3 to 50) and (2.6 to 8.0) for footing size (100×200 mm) and (200×400 mm), respectively. Meanwhile, for embedded footing, the ratio becomes (4.0 to 21.3) and (17.0 to >> 1.0) for footing size (100×200 mm) and (200×400 mm), respectively. This response is attributed to high resistanceof soil to compression that results from the increase in soil stiffness.

Furthermore, the results show that the settlement of dry loose sand is greater than that of dry dense sand with a ratio (2.6 to 50.0) and (4.0 to >> 1.0) for footing placed at the surface and embedded, respectively.

In addition to the above-mentioned remarks, it was found that the settlement of the footing is reduced when the contact area of the footing increases. For dry loose sand models, the ratio between the settlement of footing size (200×400 mm) to footing size (100×200 mm) is ranging from (0.0 to 0.28) and (0.13 to 0.50) for footing placed on the surface and embedded in soil, respectively. Meanwhile, for dry dense sand models,the ratio becomes (0.14 to 0.83) and (0.0 to 0.38) for footing placed at the surface and embedded in soil, respectively.

For saturated dense sand models, the ratio between the total settlement of dry dense sand models to saturated sand models is ranging from (0.00 to 0.22) and (0.0 to 0.56) for footing placed on the surface and embedded in soil, respectively. This behavior is attributed to the reduction in the bearing pressure intensity applied on the soil when contact area of the footing increased providing the force applied to the footings of different sizes is the same.

13. The displacement amplitude-time history

The displacement amplitude of footing (Az) was measured for all the tested models. The displacement was measured by using vibration meter. This device is used with computer interface software. The data can be directly taken from the software, or the data can be taken as displacement amplitude-time (Az-t). The latter approach was followed for the sake of illustration.

The test results of the displacement amplitude with time are illustrated in Figs. 10 to 21. The relationship of the (Az-t) was established as the measured amplitude versus the time of reading. From the test results, it can be seen that the trend of the test results is not unique for all the tests. This may be attributed to the test conditions and the dynamic response of soil. In addition, this trend is clear for the loose state models, while for dense state, the trend seems to be unique for all the tested models.

In most engineering practice, it is always desirable to get the maximum displacement amplitude of motion. Hence, the maximum values are picked up and presented in Figs. 22 to 27, and summarized in Table 2. The figures establish the maximum displacement amplitude versus the operating frequency (ω_r). For the sake of comparison, Tables 4 and 5 are prepared. These tables represent the comparison results between different models and this comparison is expressed as ratios. From examining the tests result, the following conclusions are drawn:

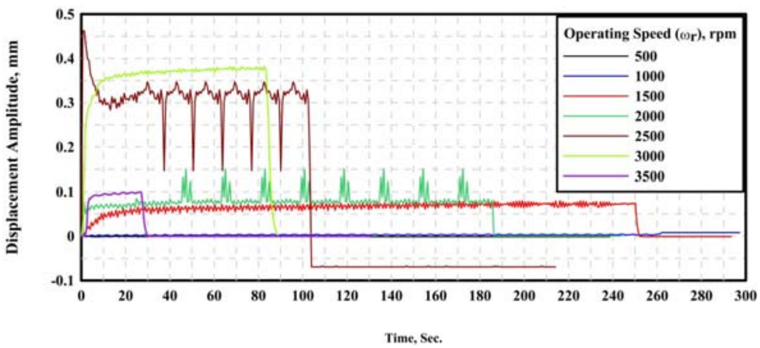

Fig. 10 The displacement amplitude versus time for DL1020S model

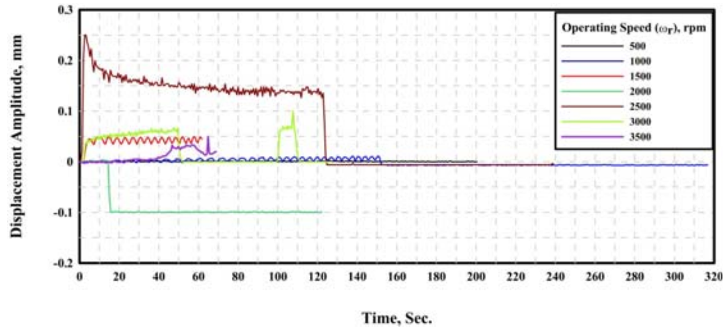

Fig. 11 The displacement amplitude versus time for DL2040S model

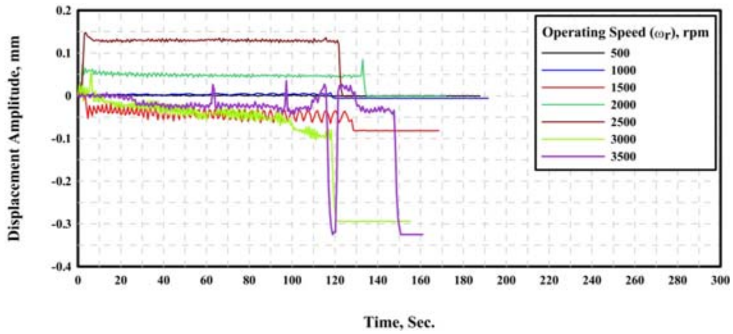

Fig. 12 The displacement amplitude versus time for DL1020E model

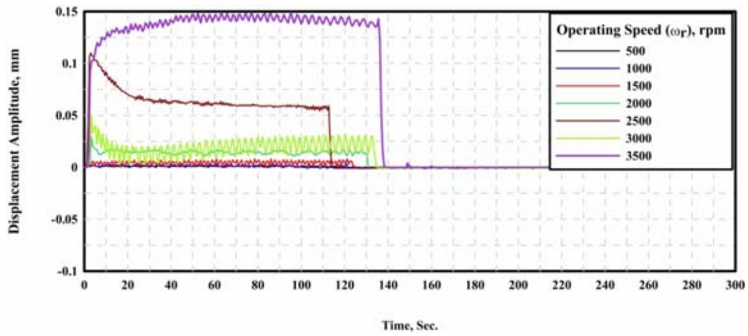

Fig. 13 The displacement amplitude versus time for DL2040E model

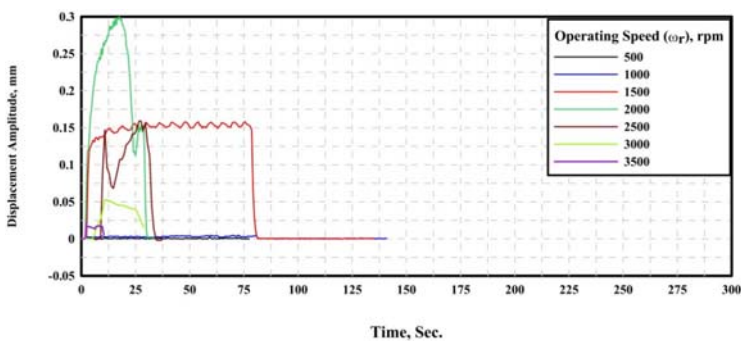

Fig. 14 The displacement amplitude versus time for DD1020S model

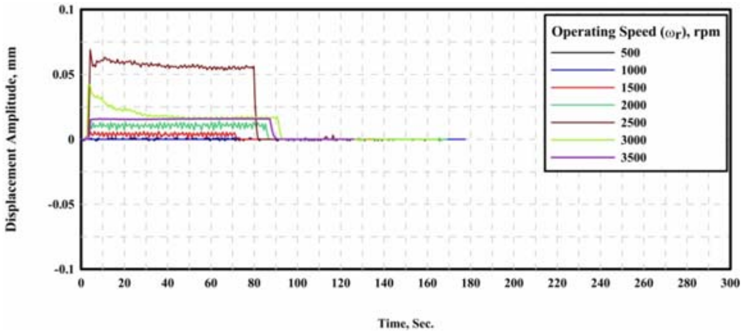

Fig. 15 The displacement amplitude versus time for DD2040S model

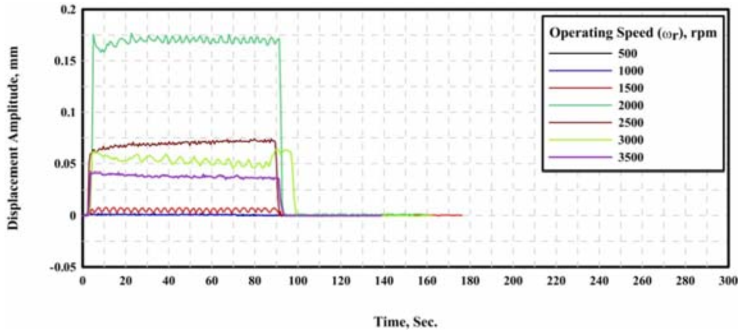

Fig. 16 The displacement amplitude versus time for DD1020E model

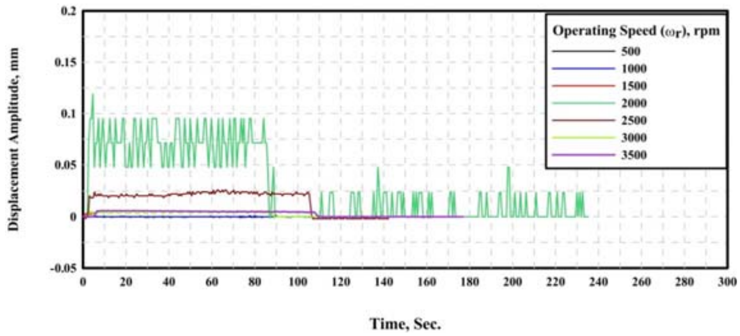

Fig. 17 The displacement amplitude versus time for DD2040E model

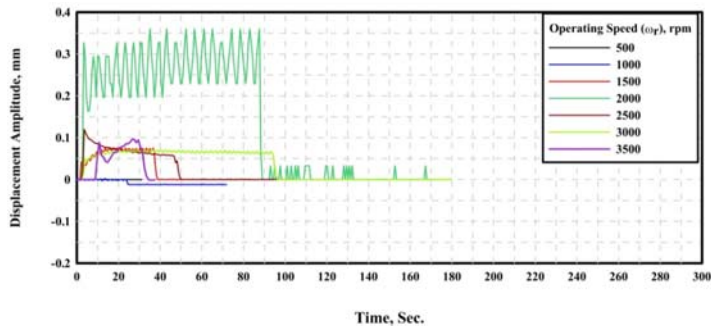

Fig. 18 The displacement amplitude versus time for SD1020S model

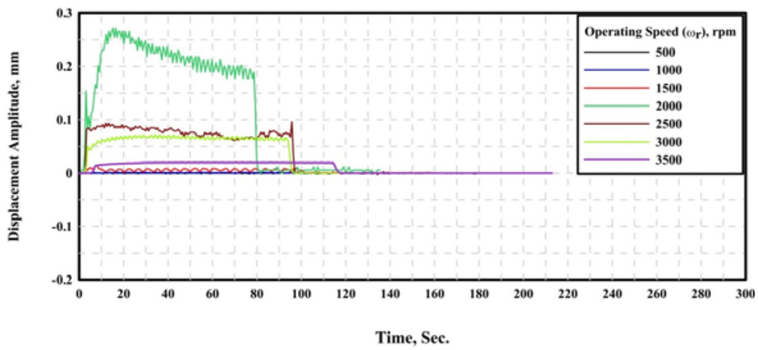

Fig. 19 The displacement amplitude versus time for SD2040S model

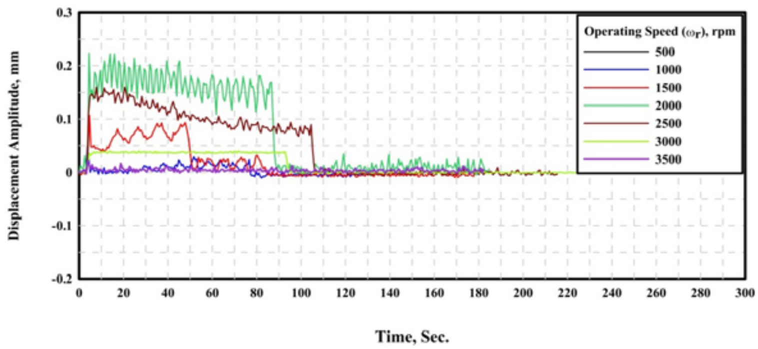

Fig. 20 The displacement amplitude versus time for SD1020E model

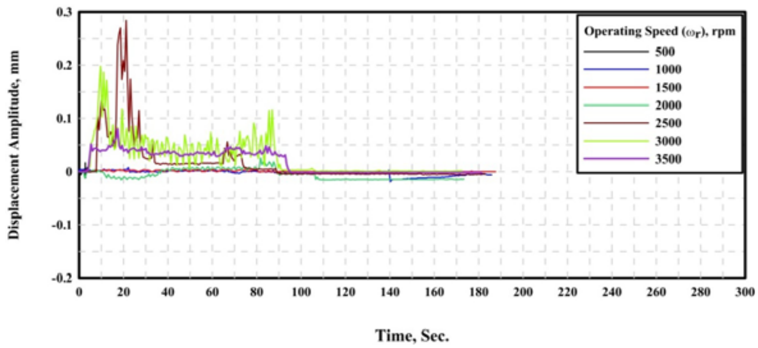

Fig. 21 The displacement amplitude versus time for SD2040E model

• The maximum values of displacement amplitude (Az) for saturated dense sand models are almost more than those for dry dense sand models with a ratio ranging from (1.00 to 11.0) and (1.10 to 19.17) for surface and embedded footing, respectively. This behavior is attributed to the increase in the pore water pressure during dynamic load that causes reduction in the inter-particle forces between solid particles of the soil skeleton hence causing an increase in displacement response. Another reason for this behavior could be the short period during vibration that prevents solid particles from interlocking with each other to rearrange their skeleton to resist the applied dynamic loading. It is expected that for a long period of vibration, the displacement amplitudes of

Table 4 Comparison ratios between the maximum measured amplitude for different models and test conditions

ω_r rpm	$\left(\frac{DD10Z0S}{DL10Z0S}\right)$	$\left(\frac{DDZ040S}{DLZ040S}\right)$	$\left(\frac{DD10Z0E}{DL10Z0E}\right)$	$\left(\frac{DDZ040E}{DLZ040E}\right)$	$\left(\frac{DD10Z0S}{DD10Z0E}\right)$	$\left(\frac{DDZ040S}{DDZ040E}\right)$	$\left(\frac{DL10Z0S}{DL10Z0E}\right)$	$\left(\frac{DLZ040S}{DLZ040E}\right)$	$\left(\frac{SD10LZ0S}{DD10Z0S}\right)$	$\left(\frac{SDZ040S}{DDZ040S}\right)$
500	1.00	0.03	0.67	0.25	0.05	0.10	0.03	0.75	11.00	10.00
1000	0.54	0.06	0.26	0.47	2.86	0.71	1.37	5.40	0.33	3.30
1500	0.88	0.10	0.24	0.56	8.13	1.50	2.18	8.06	1.00	3.00
2000	0.99	0.94	0.98	0.97	1.74	3.02	1.72	3.10	2.42	2.34
2500	0.30	0.26	0.56	0.24	2.01	2.93	3.74	2.69	0.98	1.24
3000	0.27	0.39	0.94	0.10	0.75	6.79	2.61	1.67	1.98	2.11
3500	0.27	0.29	0.99	0.64	0.97	2.47	3.56	5.46	2.80	1.33

Table 5 Comparison ratios of the maximum amplitude of displacement for between different footing size sand depth of embedment

ω_r rpm	$\left(\frac{DL1040S}{DLZ040S}\right)$	$\left(\frac{DL10Z0E}{DLZ040E}\right)$	$\left(\frac{DD10Z0S}{DDZ040S}\right)$	$\left(\frac{DD10Z0E}{DDZ040E}\right)$	$\left(\frac{SD10Z0S}{SDZ040S}\right)$	$\left(\frac{SD10Z0E}{SDZ040E}\right)$
500	0.03	0.75	1.00	2.00	1.10	3.05
1000	0.69	2.70	6.00	1.50	0.61	4.57
1500	1.29	4.79	10.83	2.00	3.61	21.36
2000	1.66	3.00	1.74	3.03	1.80	0.97
2500	1.66	1.20	1.91	2.78	1.51	0.90
3000	1.75	1.12	1.21	10.91	1.14	0.54
3500	1.73	2.65	1.62	4.11	3.40	0.39

dry and saturated sand could converge to each other, an exception of the mentioned conclusions is noticed in footing size (100×200 mm) for surface footings at operating frequency of 500 and 1000 rpm, and embedded footing at frequencies of 3000 and 3500 rpm.

• The displacement amplitude (Az) for dry dense sand models is less than that of dry loose sand models. For footing placed at the surface, the ratio of dense sand models amplitude to loose sand models is ranging from (0.27 to 1.00) and (0.03 to 0.94) for footing size (100×200 mm) and (200×400 mm), respectively. Meanwhile, for embedded footings this ratio becomes (0.24 to 0.99) and (0.10 to 0.97) for footing size (100×200 mm) and (200×400 mm), respectively. These results are attributed to the increase in the stiffness and the modulus of elasticity of dense sandy soil that makes the soil stiffer and resist vibrations as well as to it could be attributed to the trench and sidewall effects.

• The displacement amplitude (Az) decreases when the footing is embedded inside soil medium. This means that the embedment of footing causes remarkable reduction in amplitude between dense and loose sand, this is due to the increase in damping of the soil-foundation system as well as the mobilization of the SSI due to embedment of footing. The percentage of reduction for loose sand was (22.70 to 45.97 %) and (33.33 to 87.59 %) for footing size (100×200 mm) and (200×400 mm), respectively. On the other hand, for dense sand models the reduction becomes (2.85 to 87.69 %) and (33.33 to 85.26 %) for footing size (100×200 mm) and (200×400 mm), respectively.

• For a specific model, the displacement amplitude (Az) increases slightly to a certain value of operating frequency(ω_r), and then there is a sharp increase in the values of the displacement amplitude followed by sharp decrease and then the rate of reduction decreases. To illustrate this behavior, Figs. 22 to 24 are redrawn in terms of maximum amplitude versus frequency ratio as given in Figs. 25 to 27. The general shape of the relationship between the amplitude of displacement and operating frequency can be approximated to be like a bell. This behavior is attributed to the fact that at the peak value of amplitude of displacement, the resonance frequency is achieved. In the experimental work, this happened clearly by the rising of the sound of the vibration machine. The noise of vibration at this operating speed is high and can cause uncomfortable mode during testing. At the time of experimental work, the frequency that caused this behavior was recorded as well as the time of great amplitudes was recorded during the test. From the experimental remarks and the maximum displacement amplitude obtained, it can be concluded that the maximum displacement amplitude is obtained at frequency ranging from 30 to 40 Hz. This frequency is considered as the resonance frequency and used to estimate the damping ratio.

• The displacement amplitude (Az) of the footing size (200×400 mm) is less than that of footing of size (100×200 mm). This is true for all dry models except model for dry loose sand and some of the saturated sand models. As can be seen from Table 5, for dry loose sand models, the ratio between footing size (100×200 mm) to footing size (200×400 mm) is ranging from (1.29 to 1.75) and (1.12 to 4.79) for footing placed at the surface and embedded, respectively. On the other hand, for dry dense sand the ratio becomes (1.00 to 10.83) and (1.50 to 10.91) for footing placed on the surface and embedded, respectively. Meanwhile, for saturated dense sand, the rate of reduction reduces and goes from (1.10 to 3.61) for footing placed on the surface, while the behavior of embedded footing in saturated dense sand seems to have opposite behavior to the aforementioned trend. The reduction in response for large contact area is attributed to the reduction in the stresses due to large contact area.

• The displacement amplitude (Az) of saturated soil samples exhibits the same resonance frequency, except for sample of footing size (200×400 mm) and embedded at 5.0 cm. This is due to the presence of water within the soil particles that may require high frequency to produce resonance phenomenon.

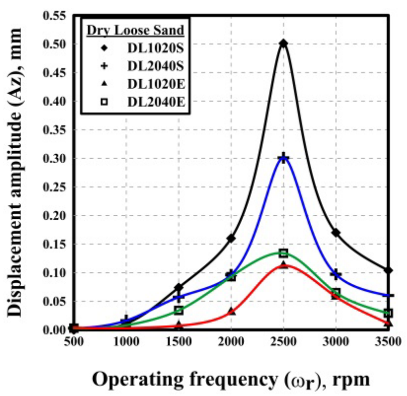

Fig. 22 The maximum displacement amplitude versus operating frequency for dry loose sand models

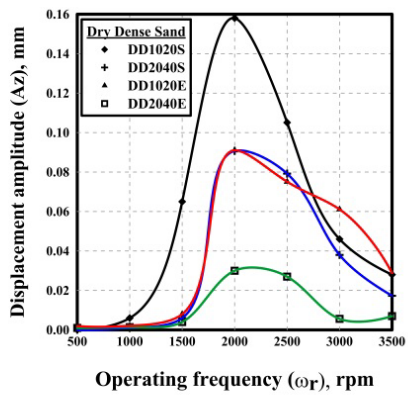

Fig. 23 The maximum displacement amplitude versus operating frequency for dry dense sand models

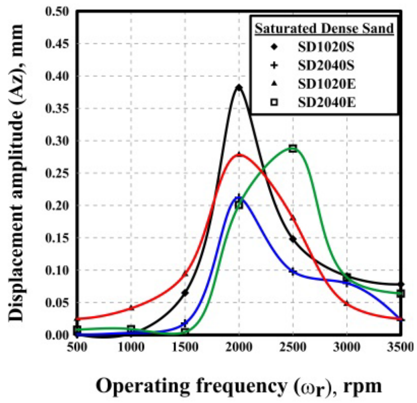

Fig. 24 The maximum displacement amplitude versus frequency ratio for dry dense sand models

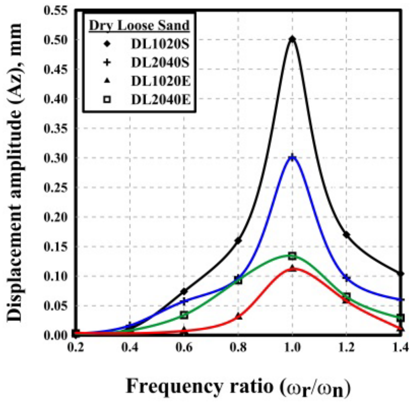

Fig. 25 The maximum displacement amplitude versus operating frequency for saturated loose sand models

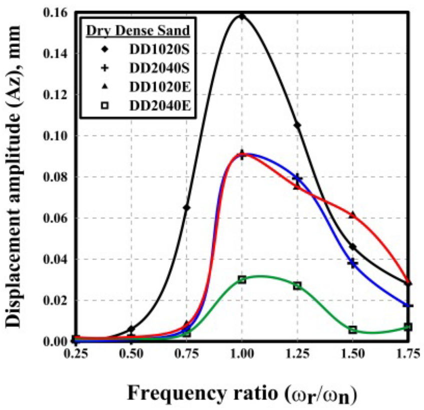

Fig. 26 The maximum displacement amplitude versus frequency ratio for dry dense sand models

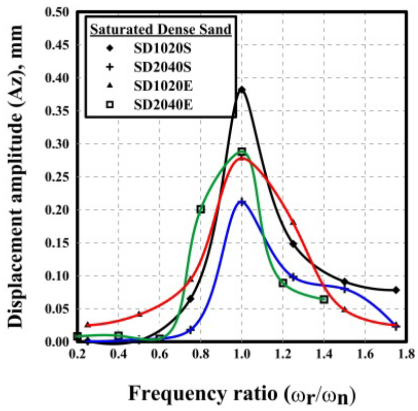

Fig. 27 The maximum displacement amplitude versus frequency ratio for saturated dense sand models

14. Conclusions

The present work, which deals with the dynamic response of machine foundations to steady state dynamic loading, clarifies the response of soil and foundation to such loading condition. The present work cannot be considered as a complete study of the response of machine foundations to dynamic loading (in addition to the data available in literature), which are restricted to the number of variables studied especially for the measurements of stresses inside soil media. Other parameters that influence the behavior of such machine foundations have not been taken into consideration in this work. Hence, the limitations within the testing program are:

- The footing is steel rectangular with aspect ratio (L/B)=2.0,
- The soil used is poorly graded sand passes sieve No. 10 (2.0 mm),
- The type of the manufactured machine is reciprocating rotating machine,
- This is done only for vertical vibration.

1. For dry and saturated conditions, the maximum amplitude of displacement decreases with

increasing the relative density of sand and contact area of footing while it increases with increasing the amplitude of loading. The maximum displacement amplitude response of the foundation resting on dry sand models is more than that on the saturated sand. The maximum displacement amplitude of footing is reduced to half when the size of footing increases to double for dry and saturated sand. The percentage of reduction of the maximum amplitude of displacement in dry sand is more than that of saturated sand.

2. The final settlement (S_t) of the foundation increases with increasing the amplitude of dynamic force, operating frequency and degree of saturation. Meanwhile, it is reduced with increasing the relative density of sand, modulus of elasticity and embedding inside soils.

3. The maximum displacement amplitude exhibits its maximum value at the resonance frequency, which is found to be about 33.34 to 41.67 Hz. The maximum values of displacement amplitude (Az) for saturated dense sand models are almost more than those for dry dense sand models with a ratio ranging from (1.00 to 11.0) and (1.10 to 19.17) for surface and embedded footing, respectively.

4. In general, embedment of footing in sandy soils leads to a beneficial reduction in dynamic response (displacement and excess pore water pressure) for all soil types in different percentages accompanied by an increase in soil strength.

5. The maximum displacement amplitude exhibits its maximum value at the resonance frequency, which is found to be about 33.34 to 41.67 Hz. On the other hand, the pore water pressure increases with increasing operating frequency. The rate of increasing of the pore water pressure possesses its maximum value at the resonance frequency, after that the rate is reduced remarkably.

6. For a specific model, the displacement amplitude (Az) increases slightly to a certain value of operating frequency(ω_r), and then there is a sharp increase in the values of the displacement amplitude followed by sharp decrease and then the rate of reduction decreases.

7. The damping ratio increases by a percentage of about 4.0 to 100 % with embedment of footing inside the soil for dense and loose sand, respectively. In addition, the damping ratio of saturated sand is more than that of dry sand by a percentage of about 40.0 to 50.0 % for embedded models.

References

Al-Homoud, A.S. and Al-Maaitah, O.N. (1996), "An experimental investigation of vertical vibration of model footings on sand", *Soil Dyn. Earthq. Eng.*, **15**(7), 431-445.

American Society of Testing and Materials (ASTM) (2006), *Standard test method for specific gravity of soil solids by water pycnometer*, ASTM D854, West Conshohocken, Pennsylvania, USA.

American Society of Testing and Materials (ASTM) (2006), *Standard Test Method for Particle Size-Analysis of Soils*, ASTM D422-63 (2002), West Conshohocken, Pennsylvania, USA.

American Society of Testing and Materials (ASTM) (2006), *Standard Test Method for Maximum Index Density and Unit Weight of Soils Using a Vibratory Table*, ASTM D4253-00 (2006), West Conshohocken, Pennsylvania, USA.

American Society of Testing and Materials (ASTM) (2006), *Standard Test Method for Minimum Index Density and Unit Weight of Soils and Calculation of Relative Density*, ASTM D4254-00 (2006), West Conshohocken, Pennsylvania, USA.

American Society of Testing and Materials (ASTM) (2006), *Standard Test Method for Direct Shear Test of Soils Under Consolidated Drained Conditions*, ASTM D3080-04, West Conshohocken, Pennsylvania, USA.

American Society of Testing and Materials (ASTM) (2006), *Standard Test Method for Density and Unit Weight of Soil in Place by the Rubber Balloon Method*, ASTM D2167-01 (2004), West Conshohocken, Pennsylvania, USA.

American Society of Testing and Materials (ASTM) (2006), *Standard Test Method for Unconsolidated-Undrained Triaxial Compression Test on Cohesive Soils*, ASTM D2850-03a, West Conshohocken, Pennsylvania, USA.

American Society of Testing and Materials (ASTM) (2006), *Standard Test Method for Permeability of Granular Soils (Constant Head)*, ASTM D2434-68, West Conshohocken, Pennsylvania, USA.

American Society of Testing and Materials (ASTM) (2006), *Standard Test Method for Classification of Soils for Engineering Purposes (Unified Soil Classification System)*, ASTM D2487-06, West Conshohocken, Pennsylvania, USA.

Bhatia, K. (2009), *Foundations for Industrial Machines: Handbook for Practicing Engineers*, CRC.

Boumekik, A., Belhadj-Mostefa, S. and Meribout, F. (2010), "Experimental analysis of the dynamic stress distribution at the soil foundation interface", *Asian J. Civ. Eng. (Building and Housing)*, **11**(5), 575-583.

Chowdhury, I. and Dasgupta, S.P. (2010), *Dynamics of Structure and Foundations-A Unified Approach: 2. Applications*, CRC Press.

Christian, J.T. and Hall, J.R. (1982), "Soil-structure interaction problems", *Proceedings of the Fourth International Conference on Numerical Methods in Geotnechanics*, Edmonton, Canada.

Fattah, M.Y., Salman, F.A. and Nareeman, B.J. (2011), "Numerical simulation of triaxial test in clayey soil using different constitutive relations", *Adv. Mater. Res.*, **243-249**, 2973-2977, Trans Tech Publications, Switzerland.

Fattah, M.Y., Al-Neami, M.A. and Jajjawi, N.H. (2013), "Prediction of liquefaction potential and pore water pressure beneath machine foundations", *Central Eur. J. Eng.*, **4**(3), 226-249.

Han, Y. (2010), "Dynamic analysis for foundation of vibrating equipment considering soil-structure interaction", *Soil Dyn. Earthq. Eng.*, Geotechnical Special Publication No. 201, ASCE, 71-76.

Livaoglu, R. and Dogangun, A. (2007), "Effect of foundation embedment on seismic behavior of elevated tanks considering fluid-structure-soil interaction", *Soil Dyn. Earthq. Eng.*, **27**(9), 855-863.

Lu, X. and Cui, P. (2004), "The liquefaction and displacement of highly saturated sand under water pressure oscillation", *Ocean Eng.*, **31**(7), 795-811.

Manyyear Technology Company Ltd. (2010), www.manyyear.com.

Messioud, S., Sbartai, B. and Dias, D. (2016), "Seismic response of a rigid foundation embedded in a viscoelastic soil by taking into account the soil-foundation interaction", *Struct. Eng. Mech.*, **58**(5), 887-903.

Omidvar, M., Iskander, M. and Bless, S. (2012), "Stress-strain behavior of sand at high strain rates", *Int. J. Impact Eng.*, **49**, 192-213.

Piezo Film Sensors Technical Manual (2008), Measurement Specialties, Inc., www.meas-spec.com

Ramesh, H.N. and Kumar. M.T. (2011), "Concepts and problems in the design of foundations subjected to vibrations", *Int. J. Geomech.*, ASCE, 312-321.

Xiaobing, L., Qingming, T., Cheng, C., Shanbing, Y. and Peng, C. (2004), "Liquefaction and displacement of saturated sand under vertical vibration loading", *Acta Mechanica Sinica*, **20**(1), 96-105.

CC